IEEE Access
Multidisciplinary ⋮ Rapid Review ⋮ Open Access Journal

Received 29 November 2023, accepted 3 January 2024, date of publication 8 January 2024,
date of current version 18 January 2024.

Digital Object Identifier 10.1109/ACCESS.2024.3351183

RESEARCH ARTICLE

Fractional Dual-Tilt Control Scheme for Integrating Time Delay Processes: Studied on a Two-Tank Level System

DIPJYOTI DAS[1], (Graduate Student Member, IEEE), SUDIPTA CHAKRABORTY[1], UTKAL MEHTA[2], (Senior Member, IEEE), AND G. LLOYDS RAJA[3], (Member, IEEE)

[1]National Institute of Technology Silchar, Silchar 788010, India
[2]Electrical and Electronics Engineering, The University of the South Pacific, Suva, Fiji
[3]National Institute of Technology Patna, Patna 800005, India

Corresponding author: Utkal Mehta (utkal.mehta@usp.ac.fj)

This work was supported by the Research Award Fund of The University of the South Pacific, Fiji.

ABSTRACT Industrial processes of time delayed integrating type require sophisticated control methods because of their non-self-regulating nature. Literature presents fractional order controllers as possible solution to this problem and there is scope for further enhancing the performance of the existing solutions. Though fractional order controllers are capable of outperforming their integer order counterparts, it is evident in literature that the former controller designs are complex and hence analytical tuning procedures for the same are scarce. Hence, this paper presents a novel predictive strategy for time-delayed integrating processes based on two fractional-order tilt-derivative ($\text{FOT}^{\alpha}\text{D}^{1-\alpha}$) controllers. These controllers are analytically designed with only two tunable parameters. These tuneables are computed using gain- and phase-margin specifications. In contrast to the previous methods, the presented scheme is more capable of eliminating input-load disturbances without adding complexity in terms of tunable parameters. In addition to the investigations carried out using three difficult benchmark plant models, the present design is also experimentally validated using a two-tank level control system to vindicate its efficacy. Through robust stability analysis, it is shown that the suggested strategy is capable of achieving stable closed-loop responses amid upto 50% perturbation in plant parameters.

INDEX TERMS Fractional-order tilt derivative controller, integrating processes, time delay, gain margin, phase margin, robustness.

I. INTRODUCTION

Integrating process or non-self-regulating process generates an unbounded output for a bounded input and may result in actuator saturation [1]. Distillation columns, boiler steam drums, level loops, jacketed CSTRs, batch operations, and bioreactors are a few examples of well-known industrial processes [2]. PID controllers and their equivalents are still used in the majority of industrial loops because of their simple construction and lack of intricate design [3], [4], [5]. Among PID variants, 2DOF PID is one of the most explored options in recent times. An I-PD control law was recommended to regulate an integrating process in [1] and [6]. Applying the centroid of the stability region, the PI-PD controller was designed in [7]. In [3], an all-PD control law based on GM-PM criteria was explored. A PI-PD controller was developed in [8] using M_S constraints and moment-matching. Another PI-PD control law based on GM-PM and M_S constraints was suggested in [9]. An optimal I-PD controller was designed in [10]. Based on frequency loop shaping and GM-PM specifications, a 2DOF PID-PD control structure was explored in [2].

The associate editor coordinating the review of this manuscript and approving it for publication was Sajid Ali.

TABLE 1. List of abbreviations and symbols.

Abbreviations/ Symbols	Definition
DOF	Degree of Freedom
PID	Proportional-Integral Derivative
TID	Tilt-Integral-Derivative
FOPID	Fractional Order PID
IOC	Integer Order Controller
FOC	Fractional Order Controller
FOTID	Fractional Order TID
GM	Gain Margin
PM	Phase Margin
M_S	Maximum Sensitivity
IMC	Internal Model Control
CSTR	Continuously Stirred Tank Reactor
FOTDD	Fractional-order tilt double derivative
FOT$^{\alpha}$D$^{1-\alpha}$	Fractional-order tilt-derivative
C	setpoint tracking FOT$^{\alpha}$D$^{1-\alpha}$ controller
C_d	disturbance rejection FOT$^{\alpha}$D$^{1-\alpha}$ controller
P	Plant model
K and L	Gain and Time delay of plant model
P_m	Delay-free part of plant model
K_{t1} and K_{d1}	Tilt and derivative gains in C
K_{t2} and K_{d2}	Tilt and derivative gains in C_d
α_1 and α_2	Fractional order parameter in C and C_d
MK_{S2}, M_{S2}	Maximum sensitivities of servo and regulatory loops
γ_s and ϕ_s	GM, PM of servo loop
γ_r and ϕ_r	GM and PM of regulatory loop
λ_1, λ_2	Closed-loop time constant of servo and regulatory loops
ω_{pcs},ω_{gcs}	Phase and gain crossover frequencies of servo loop
ω_{pcr},ω_{gcr}	Phase and gain crossover frequencies of regulatory loop

It is proven that integer-order controllers (IOCs) are favourite for their simplicity in tuning, making them easier to implement in practical applications. However, IOCs fall short in their performance. Recent years have seen a substantial increase in the popularity of fractional-order PID (FOPID) controllers due to their capacity to enhance performance and robustness compared to PID [11], [12], [13]. Trivedi and Padhy [14] used an indirect FOC based on the IMC method. A FO PI-PD control rule was developed for stable and unstable systems in [15]. The quadrotor drones can be controlled as a double integrating system with high nonlinearity in nature using a simple PI$^{\lambda} - D$ structure [16], [17]. Further, an optimal FOI$^{\lambda}$D$^{1-\lambda}$ was designed in [18] for time-delayed integrating processes based on a complex-root-boundary analysis. In [19], a non-singular terminal sliding mode controller using a PID-based fractional disturbance observer was described. The fractional-order tilt double derivative controller (FOTDD) design reported in [20] is based on modified IMC theory. It is extended for unstable processes in [21]. For mitigating frequency deviation in power system (PS), a FO integral-tilt derivative controller with filter (FOI-TDN) was employed in [22]. To achieve load frequency control in hybrid PS, the FO cascaded integral derivative tilt controller was designed in [23]. For frequency control in multimicrogrid, an ITD controller was developed in [24]. Advanced control methods such as neural network [25] and fuzzy logic [26] involve complex computations. In practice, simple cotrol strategy are prefered [18].

Addressing this literature gap, the goal is to design a FOC with a streamlined structure, requiring fewer tuning parameters than popular FOPID. Also, the new controller should be simple to implement in real-time applications and offer superior performance with robustness. Among the various subsets of PID, TID is more advantageous due to the 'tilt' term extending the controller's overall bandwidth [27]. Also, fractional order controllers can yield better performance-robustness trade-off [18]. Hence, combining the merits of both tilt and fractional order controllers is worthwhile. However, the recently reported tri-parametric FOID controller design [18] failed to reject input-load disturbance. It is worth mentioning that the bulk of FOPID or TID designs reported in the literature are complex due to the requirement of three to five tuning parameters. Additionally, most designs do not include the analytical or absolute tuning procedure. In some cases, the

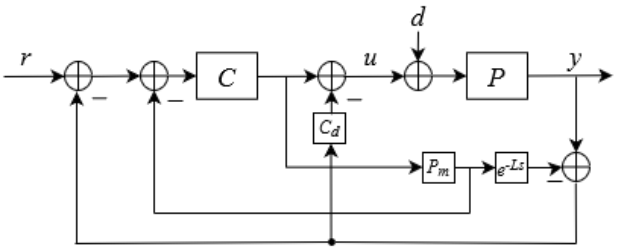

FIGURE 1. A fractional dual-tilt control scheme.

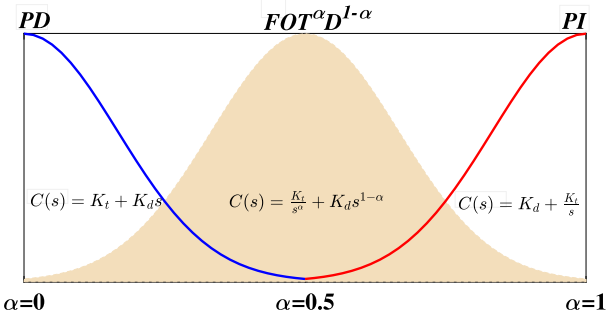

FIGURE 2. FOT$^{\alpha}$D$^{1-\alpha}$ behaviours.

fractional order is also heuristically tuned, thereby making the procedure complex [28]. Given the foregoing details, the main contributions of this work can be summarised as follows:

- By combining the merits of both tilt and fractional order controllers, a new method of designing fractional-order tilt-derivative (FOT$^{\alpha}$D$^{1-\alpha}$) controller with only two tunable parameters is recommended.
- Two such FOT$^{\alpha}$D$^{1-\alpha}$ controllers with identical parameters are employed in a predictive control structure.
- Controller parameters are analytically computed using GM-PM specifications.
- Although the proposed predictive structure has four tuning parameters, the servo and regulatory controllers are identical in contrast to typical 2DOF schemes. This makes the method further simplified with only two tuning parameters.
- Contrary to the FOID controller design of [18], the present scheme is capable of eliminating input-load disturbance effectively.
- The performance and robustness of a closed-loop system are widely acknowledged to be inversely correlated [29]. However, the present control scheme is set up in a way that strikes a good trade-off between the two.
- The suggested design is experimentally validated on a two-tank level control system.

The rest of this draft is arranged as follows: Proposed predictive control structure and transfer function of controllers are brought forth in Section II. Analytical design of FOT$^{\alpha}$D$^{1-\alpha}$ controllers are carried out in Section III. Section IV is devoted to the discussion of simulation results, whereas experimental validation of the proposed scheme is carried out in Section V. Conclusions are presented in Section VI.

II. CONTROL STRUCTURE AND THEORETICAL FORMULATIONS

Figure 1 shows a Smith predictor-based proposed control structure where P is the actual plant to be controlled and C and C_d are the servo tracking and disturbance rejection controllers, respectively. Here, P_m is the delay-free plant model, r is the set-point to the system, y is the process output, u is the control efforts generated by the controller and d is the disturbance input. The elimination of the time delay L from the closed-loop characteristic equation and also the ability to anticipate the future value of the controlled variable using a plant model are the main advantages of a predictive structure. In this work, both C and C_d are identical controllers and can be expressed as below.

$$C(s) = \frac{K_{t1}}{s^{\alpha_1}} + K_{d1}\, s^{1-\alpha_1} \tag{1}$$

$$C_d(s) = \frac{K_{t2}}{s^{\alpha_2}} + K_{d2}\, s^{1-\alpha_2} \tag{2}$$

where $K_{t1,2}$ and $K_{d1,2}$ terms denote the tilt and derivative gains, respectively. The orders $\alpha_{1,2}$ and $1-\alpha_{1,2}$ are the non-zero fractional orders and $\alpha_{1,2} \in (0, 1)$. As illustrated in Figure 2, choosing $\alpha_{1,2} = 0$ transforms $C(s)$ into a classical PD, whereas choosing $\alpha_{1,2} = 1$ results in a classical PI. Consequently, the FOT$^{\alpha}$D$^{1-\alpha}$ yields a trade-off between PD and PI control actions. Changes in set-point and disturbances elicit two distinct responses from a control system: the servo response, triggered by set-point adjustments, and the regulatory response, activated in response to disturbances. The transfer functions for the servo $G_{r,y}(s)$ and regulatory $G_{d,y}(s)$ responses can be obtained from Figure 1 as:

$$G_{r,y}(s) = \frac{KC(s)e^{-Ls}}{s + KC(s)} \tag{3}$$

$$G_{d,y}(s) = \frac{K[s + KC(s)(1 - e^{-Ls})]e^{-Ls}}{[s + KC(s)][s + KC_d(s)e^{-Ls}]} \tag{4}$$

where, K and L denotes system gain and delay of the process P, respectively.

Now from (4), it can be concluded that zero steady-state error in regulatory response is possible only with $C_d(s) \neq 0$. Let us take servo and regulatory loops comprising plant P and controller (C or C_d). The respective maximum sensitivities (M_{S1} and M_{S2}) are the inverse of the minimal distance from the point $(-1, 0)$ to the Nyquist plot. Accordingly, the M_S for the servo and regulatory loops are as follows:

$$M_{S1} = \max||\frac{1}{1 + P(j\omega)C(j\omega)}||_{\infty} \tag{5}$$

$$M_{S2} = \max||\frac{1}{1 + P(j\omega)C_d(j\omega)}||_{\infty} \tag{6}$$

As M_S is inversely proportional to the distance from the point $(-1, 0)$ to the Nyquist plot, the system stability

deteriorates with increased maximum sensitivity and vice-versa. To ensure stability, the phase crossover frequency (ω_{pc_s}) must be greater than and gain crossover frequency (ω_{gc_s}). Similarly, for the regulatory loop, $\omega_{pc_r} > \omega_{gc_r}$. From the crossover frequencies, the gain and phase margins for the servo (γ_s and ϕ_s) and regulatory (γ_r and ϕ_r) loops can be obtained. These stability margins are related to M_S as follows:

$$M_{S1} < \frac{\gamma_s}{\gamma_s - 1}, \quad M_{S1} < \frac{1}{2\sin(\frac{\phi_s}{2})} \tag{7}$$

$$M_{S2} < \frac{\gamma_r}{\gamma_s - 1}, \quad M_{S2} < \frac{1}{2\sin(\frac{\phi_r}{2})} \tag{8}$$

III. PROPOSED CONTROLLER DESIGN

The controller is designed based on an approximated pure integrating model with a time delay. However, as seen in Figure 1, the actual plant $P(s)$ may be a higher-order integrating type. Both the servo tracking controller (C) and disturbance rejection controller (C_d) are designed independently using GM-PM specifications. As C_d will come into existence only when there is a disturbance affecting the system, it allows both controllers to be designed independently.

A. DESIGN OF SERVO-TRACKING CONTROLLER

Let us consider a pure integrating plant model with a time delay as

$$P_m(s)e^{-Ls} = \left(\frac{K}{s}\right)e^{-Ls} \tag{9}$$

where K and L are the process gain and time delay, respectively. Following the internal model approach [30], the IMC controller $Q(s)$ is written as

$$Q(s) = (P_m^-(s))^{-1}F(s) = (P_m^-(s))^{-1}\frac{1}{\lambda_1 s + 1} \tag{10}$$

where λ_1 is the adjustable parameter of IMC filter $F(s)$ and $P_m^-(s)$ is the inverse of the invertible part of the plant model. As per the IMC principle, the servo controller $C(s)$ is obtained as

$$C(s) = \frac{Q(s)}{1 - P_m(s)Q(s)}. \tag{11}$$

Now, putting (9) and (10) in (11), one obtains,

$$C(s) = \frac{Ls + 1}{K(\lambda_1^2 s + 2\lambda_1)} \tag{12}$$

To convert (12) into a structured form, the first-order Maclaurin series expansion is applied as given below:

$$C(s) = C(0) + sC'(0) \tag{13}$$

where, $C(0) = \frac{1}{2K\lambda_1}$ and $C'(0) = \frac{L}{2K\lambda_1} - \frac{1}{4K}$.
Now from (13), it can be seen that there is only one tuning parameter. So, we can not impose both the GM and PM (γ_s and ϕ_s) at a time. So, $1/s^{\alpha_1}$ term is multiplied in (13) and hence we get

$$C(s) = \left[C(0) + sC'(0)\right]\frac{1}{s^{\alpha_1}} = \frac{C(0)}{s^{\alpha_1}} + C'(0)s^{1-\alpha_1} \tag{14}$$

where, $K_{t1} = C(0)$ and $K_{d1} = C'(0)$. As it can be seen that this multiplication converts the controller into a fractional-order tilt $\mathrm{FOT}^{\alpha_1}\mathrm{D}^{1-\alpha_1}$. As per expression (14), there are two unknown parameters λ_1 and α_1. Let us calculate using the well-adopted GM-PM specifications. Assuming $P(s) = G_m(s)e^{-Ls}$, the GM-PM equations of the open loop transfer function $G_{servo}(s) = P(s)C(s)$ can be computed as given below:

$$\phi_s = arg[P(j\omega_{gc_s})C(j\omega_{gc_s})] + \pi \tag{15}$$

$$|P(j\omega_{gc_s})C(j\omega_{gc_s})| = 1 \tag{16}$$

$$\gamma_s = \frac{1}{|P(j\omega_{pc_s})C(j\omega_{pc_s})|} \tag{17}$$

$$arg[P(j\omega_{pc_s})C(j\omega_{pc_s})] + \pi = 0 \tag{18}$$

where ω_{pc_s} and ω_{gc_s} are the respective crossover frequencies for the user-defined γ_s and ϕ_s. Substituting (9) and (14) in (15)-(18), we get

$$\phi_s - \frac{\pi}{2} + L\omega_{gc_s} + \frac{\pi}{2}\alpha_1 - \arctan\left(\frac{C'(0)\omega_{gc_s}}{C(0)}\right) = 0 = F_1 \tag{19}$$

$$\frac{K}{(\omega_{gc_s})^{1+\alpha_1}}\sqrt{(C(0))^2 + (C'(0)\omega_{gc_s})^2} - 1 = 0 = F_2 \tag{20}$$

$$\gamma_s - \frac{(\omega_{pc_s})^{1+\alpha_1}}{K\sqrt{(C(0))^2 + (C'(0)\omega_{pc_s})^2}} = 0 = F_3 \tag{21}$$

$$\frac{\pi}{2} - L\omega_{pc_s} - \frac{\pi}{2}\alpha_1 + \arctan\left(\frac{C'(0)\omega_{pc_s}}{C(0)}\right) = 0 = F_4 \tag{22}$$

As equations (19)-(22) have non-linear terms, they are difficult to solve analytically. Therefore, MATLAB 'fslove' function is utilised to solve those non-linear equations simultaneously with the following objective function,

$$J = \min_{(K_{t1}, K_{d1}, \omega_{pc_s}, \omega_{gc_s})} [{F_1}^2 + {F_2}^2 + {F_3}^2 + {F_4}^2]. \tag{23}$$

It is to note that the best selection is obtained by choosing $J < \sigma$, where σ is a very small value.

B. DESIGN OF DISTURBANCE REJECTION CONTROLLER

From Figure 1, the open loop transfer function involving the disturbance rejection controller is written as

$$G_{dist}(s) = P(s)C_d(s) \tag{24}$$

By replacing $C(s)$ with $C_d(s)$ and repeating the steps from (15)-(22), $C_d(s)$ can be designed with the same GM and PM (γ_s and ϕ_s). Hence, $K_{t1} = K_{t2}$, $K_{d1} = K_{d2}$, $\lambda_1 = \lambda_2$ and $\alpha_1 = \alpha_2$. However, suppose the disturbance rejection performance is not satisfactory. In that case, $C_d(s)$ can also be designed for different GM and PM (γ_r and ϕ_r), resulting in different controller parameters from that of $C(s)$.

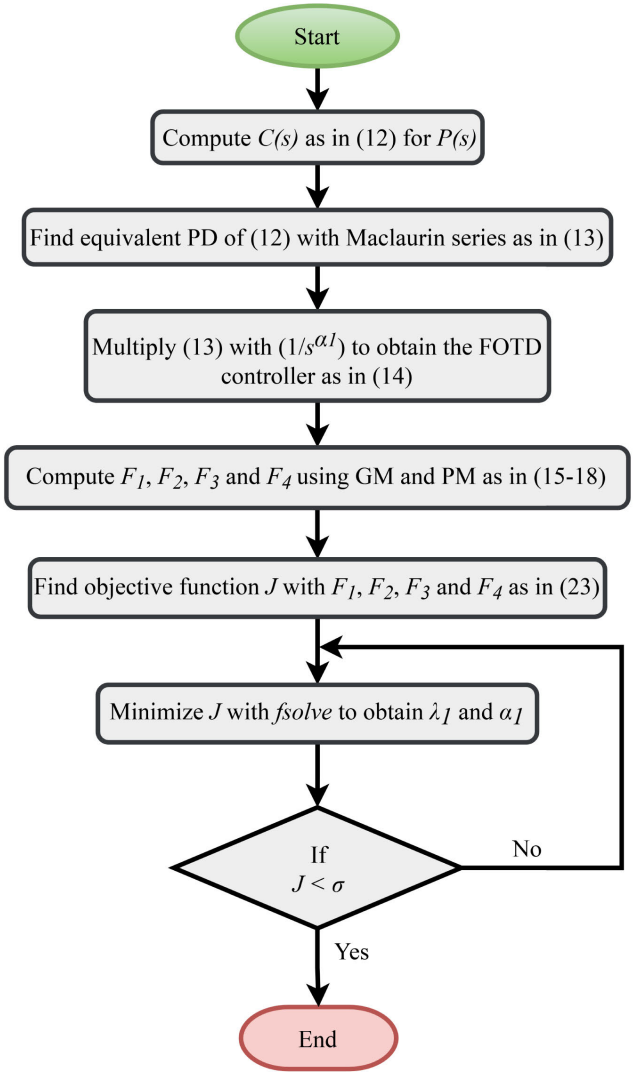

FIGURE 3. Steps to obtain parameters.

C. CONTROLLER TUNING SUMMARY

A step-by-step procedure to design the proposed controller and to obtain the tuning parameters are summarized in the flow-chart shown in Figure 3.

IV. RESULTS AND DISCUSSIONS

An investigation was conducted on three challenging benchmarks integrating processes from the literature. The controller is designed for GM= 3, PM= 60° and a derivative filter for the D-part is selected as $\frac{1}{(0.5s+1)}$ throughout the manuscript; however, these choices can be altered as per the requirements.

A. EXAMPLE-1: HIGHER ORDER INTEGRATING PROCESSES

Let us consider a higher order integrating process studied in [6] as, $P(s) = \frac{e^{-2s}}{s(s+1)(0.5s+1)(0.25s+1)}$. For this process, Peker and Kaya [6] reported an I-PD controller along with a lead-lag filter with controller parameters as $K_p = 0.2570$,

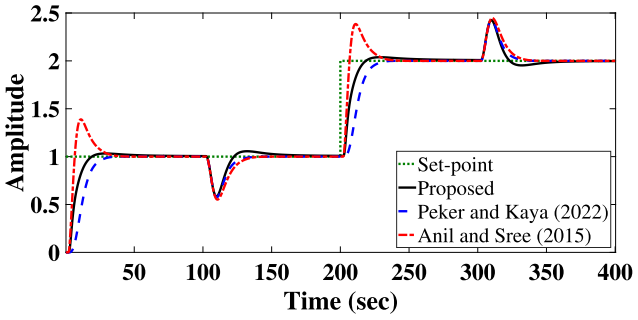

FIGURE 4. Nominal responses of example-1.

$T_i = 12.9525$, $T_d = 3.2148$, $a = 1.3337$ and $c = 3.1877$. For this same process, A PID with a lead-lag filter was suggested by Anil and Sree [31] with the following settings: $K_p = 0.2370$, $T_i = 14.4608$, $T_d = 1.5596$, $\alpha = 0.9996$ and $\beta = 1.2888$. For the proposed design, the plant is approximated as $P(s) \approx e^{-3.75s}/s$ for controller design purposes. Following the proposed design method summarized in Figure 3, $\lambda_{1,2} = 3.9574$ and $\alpha_{1,2} = 0.1218$, are obtained. The resulting controllers are $C(s) = C_d(s) = \frac{0.1263}{s^{0.1218}} + 0.2238s^{0.8782}$. Dynamic responses of the proposed design are compared with that of [6] and [31]. The simulation is run with a variable set-point of 1 at 0 sec and another step change at 200 sec. The load disturbance occurs with $d = -0.1$ at 100 sec and $d = +0.1$ at 300 sec. Figure 4 exhibit the nominal responses obtained using the unperturbed $P(s)$ mentioned above. The aforementioned figure indicates that the proposed approach demonstrates superior servo and regulatory responses compared to existing designs in terms of overshoot-free responses during setpoint changes and faster settling time while rejecting disturbances. Figure 5 illustrates the control efforts corresponding to Figure 4, thereby showcasing a notably smooth control action for the proposed method compared to its contemporaries. In contrast, the control efforts of Anil and Sree [31] shows undesirable initial kicks during setpoint changes. To evaluate robustness, a 30% perturbation is simulated in the K and L of the plant model. The resulting responses are depicted in Figure 6 along with their corresponding control efforts in Figure 7. Robustness of the present design is evident from Figures 6 and 7 as it yields superior closed-loop performance and smooth control action amid perturbations. Especially, it is worth noticing that the proposed design results in less oscillations and overshoot compared to that of Anil and Sree. Furthermore, resilience to noise is analysed by simulating a band-limited noise with a power of 0.001 at the output. The outcomes, displayed in Figures 8 and 9, highlight that the proposed design is less susceptible to noise compared to existing designs.

B. EXAMPLE-2: NON-LINEAR JACKETED CSTR

Most chemical process industries utilised the CSTRs to mix two or more reactants at a specific temperature while a catalyst was present. Because of the non-linear relationship

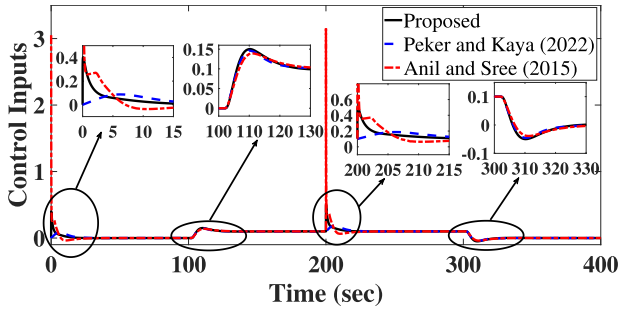

FIGURE 5. Nominal control efforts for example-1.

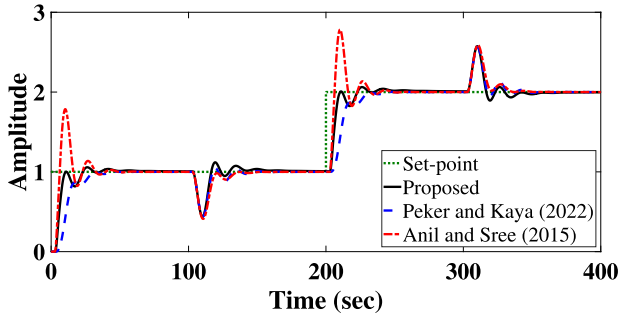

FIGURE 6. Perturbed responses with 30% increase in both process gain and delay for example-1.

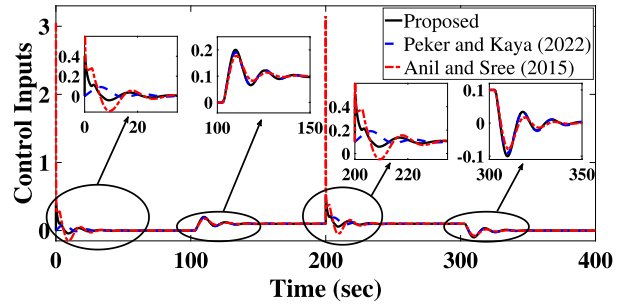

FIGURE 7. Perturbed control efforts with 30% increase in both process gain and delay for example-1.

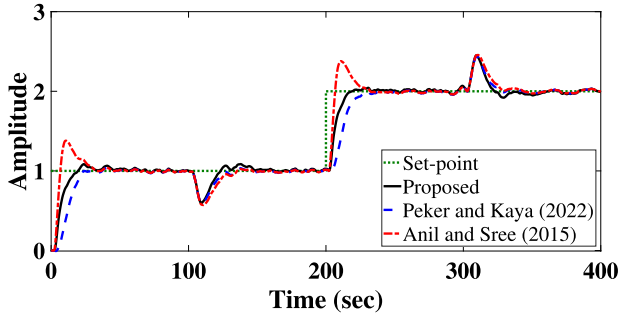

FIGURE 8. Responses with noise input for example-1.

between the manipulated and controlled variables, it is difficult to control the temperature of CSTR. Figure 10 displays a schematic diagram of a CSTR. Consider a non-linear dynamics of a Jacketed CSTR, which was recently

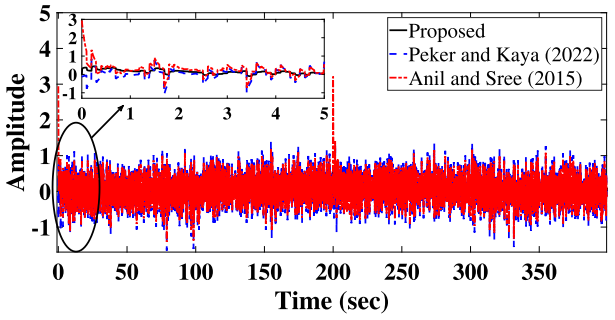

FIGURE 9. Control efforts with noise input for example-1.

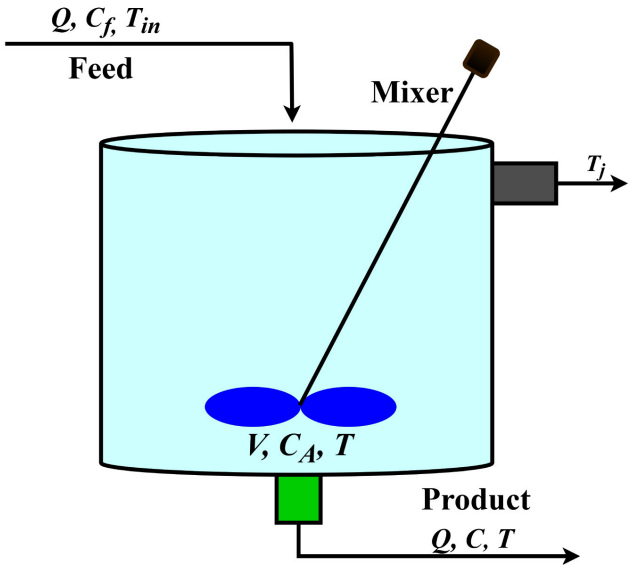

FIGURE 10. Schematic diagram of a CSTR.

explored by Mehta et al. [18] where the isothermal chemical reaction is illustrated as:

$$\frac{dC}{dt} = \frac{Q}{V}(C_f - C) - \frac{a_1 C}{(a_2 C + 1)^2} \tag{25}$$

The process is linearized as per the prescribed parameter settings [18] as, $P(s) = \frac{3.433e^{-20s}}{103.1s-1} \approx \frac{0.0333}{s}e^{-20s}$. A fractional-order integral derivative (FOI$^{\lambda}$D$^{1-\lambda}$) controller with $K_i = 0.43$, $K_d = 10.46$ and $\lambda = 0.1127$ was used by [18] for this process. To regulate the same process, Kumari et al. [32] have created a fractional order internal model control (FOIMC)-proportional controller with K_p as 1 and FOIMC as $\frac{103.1s^2+58.77s+2.433}{(3.433+34.33s)(1+16s^{1.1})}$. As per the present method summarized in Figure 3, two tuning parameters are calculated as $\lambda_{1,2} = 23.3560$ and $\alpha_{1,2} = 0.0984$. With these specifications, the controllers are designed as $C(s) = C_d(s) = \frac{0.6429}{s^{0.0984}} + 5.35s^{0.9016}$. Dynamic responses of the proposed design are compared with that of [18] and [32]. The simulation is carried out with $r = 4$ at 0 sec and $d = -1$ at 350 sec. The nominal responses are demonstrated in Figure 11 to highlight the superior servo and regulatory performances achieved by the proposed design compared to

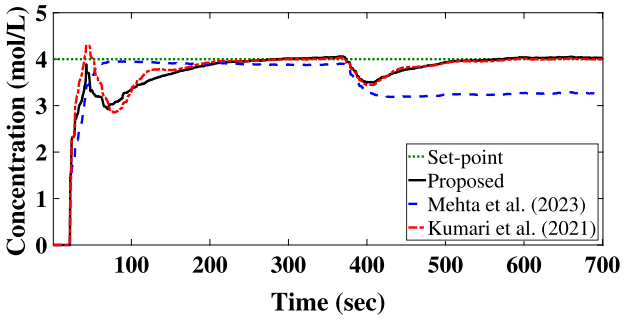

FIGURE 11. Nominal responses of example-2.

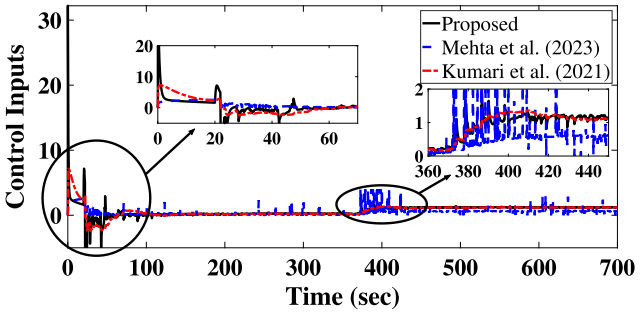

FIGURE 12. Nominal control efforts for example-2.

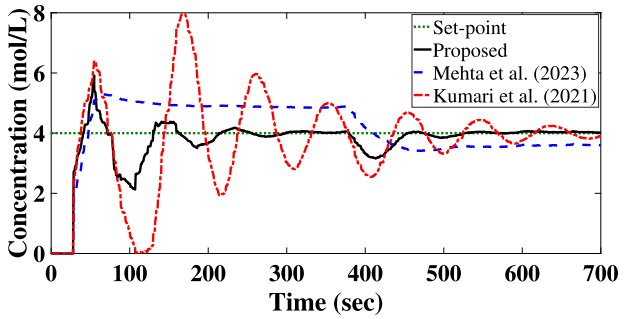

FIGURE 13. Perturbed responses with 30% increase in both process gain and delay for example-2.

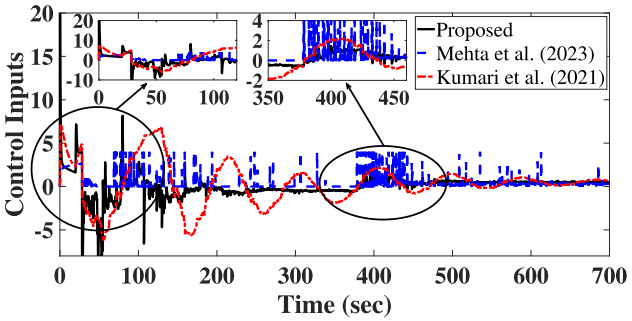

FIGURE 14. Perturbed control efforts with 30% increase in both process gain and delay for example-2.

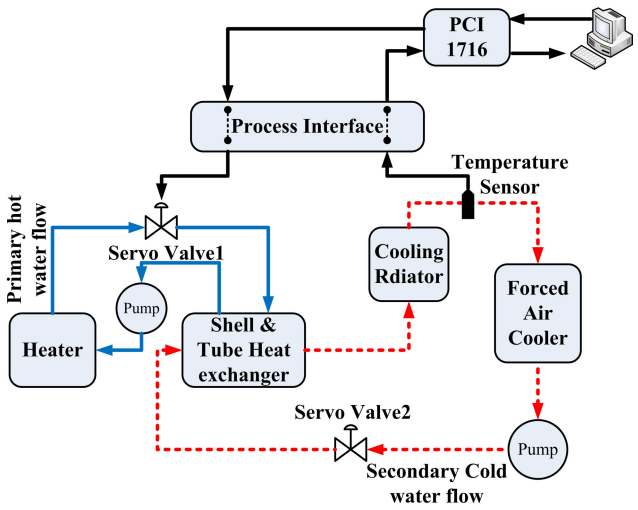

FIGURE 15. Schematic diagram of temperature control with a heat exchanger.

the existing designs. Figure 12 illustrates the corresponding control efforts, showcasing a relatively smooth control action than seen in existing designs. To assess robustness, a 30% perturbation is simultaneously simulated in both process gain and delay. The resulting responses and control efforts are displayed in Figures 13 and 14, respectively. Observing these figures reveals that the proposed design maintains enhanced servo and regulatory performances with smooth control action amid perturbations. In contrast to the proposed design, the triparametric controller of Mehta et al. [18] fails to reject the input load disturbances.

C. EXAMPLE-3: HEAT EXCHANGER

A temperature control loop involving the heat exchanger is studied, as shown in Figure 15. In this shell and tube heat exchanger, two flow lines exchange heat. This process was experimentally modelled in [3] as $P(s) = 0.002e^{-3s}/s$. For this process, Das et al. [9] have designed a PI-PD controller with parameters $K_p = 140.68$, $T_d = 1.45$, $K_c = 50.8647$ and $T_i = 2.6659$. The proposed design's two unknown parameters are obtained as $\lambda_{1,2} = 3.1114$ and $\alpha_{1,2} = 0.1256$ as per the flow chart given in Figure 3. With these settings, the proposed controllers are designed as $C(s) = C_d(s) = \frac{80.3497}{s^{0.1256}} + 116.0490s^{0.8744}$. Dynamic responses of the proposed design are compared with the already existing designs. The simulation is carried out with $r = 1$ at 0 sec and $d = -30$ at 80 sec. Nominal responses shown in Figure 16 highlights the superior servo and regulatory performances achieved by the present design compared to [9]. Likewise, control efforts shown in Figure 17 illustrates the relatively smooth control action achieved by the present design. For assessing robustness, a 30% perturbation is simulated simultaneously in both K and L. The resulting perturbed responses and their corresponding control efforts are displayed in Figures 18 and 19, respectively. These figures reveal that the proposed design is robust with smooth control action amid perturbations. In contrast, the design of [9] results in an unstable response for the perturbed case. Overall, the

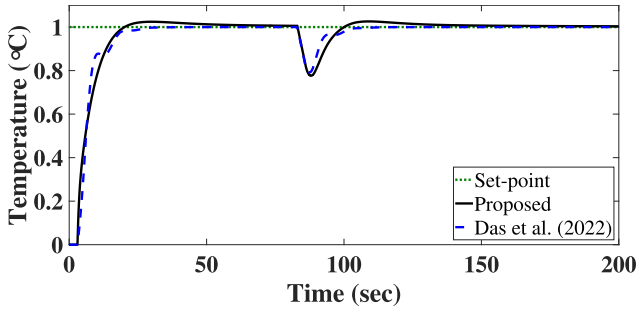

FIGURE 16. Nominal responses of example-3.

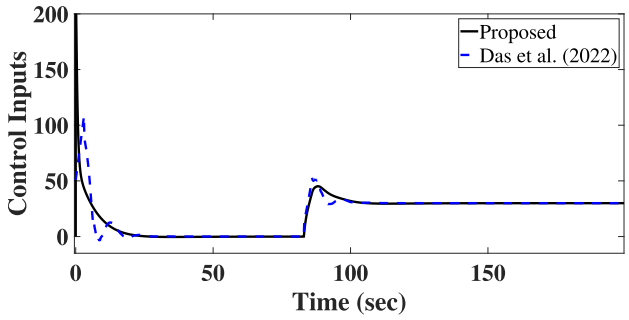

FIGURE 17. Nominal control efforts for example-3.

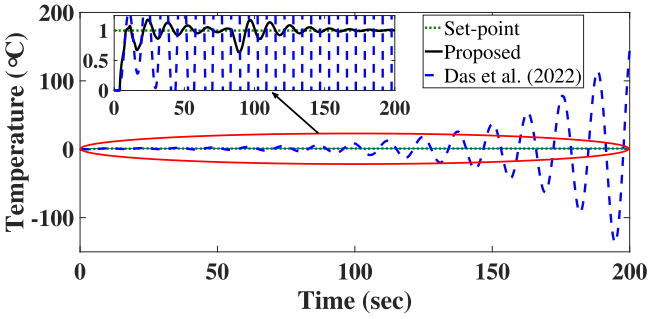

FIGURE 18. Perturbed responses with 30% increase in both process gain and delay for example-3.

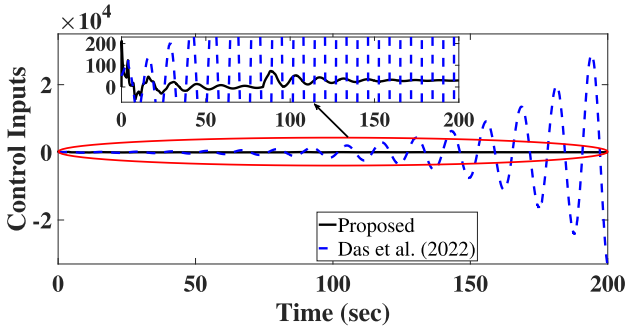

FIGURE 19. Perturbed control efforts with 30% increase in both process gain and delay for example-3.

simulation studies conducted in this sub-section reveals the superiority of the present design over [9] in terms of both performance and robustness.

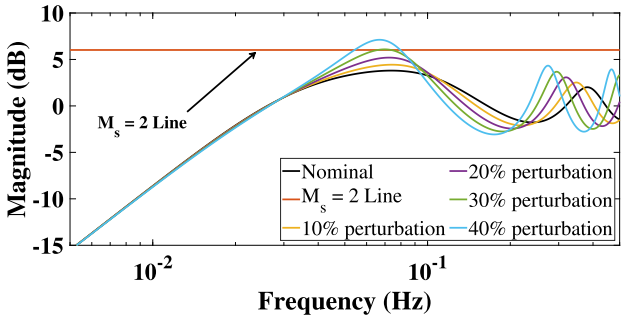

FIGURE 20. Sensitivity plots with respect to plant parameter variations for example-1.

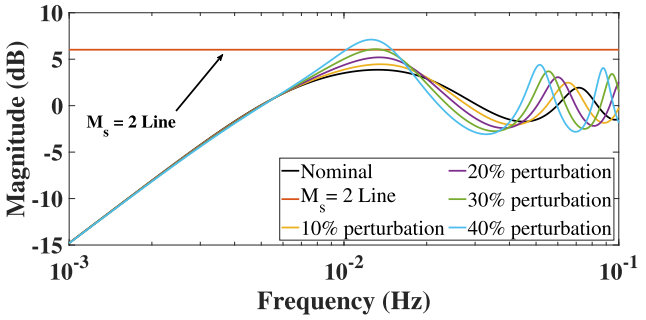

FIGURE 21. Sensitivity plots with respect to plant parameter variations for example-2.

D. ROBUSTNESS ANALYSIS

1) ROBUSTNESS CHECK USING SENSITIVITY PLOT

Although GM-PM specifications are traditional robustness metrics, they may fail to ensure a realistic sensitivity bound. To verify the sensitivity with respect to plant parameter variations, one can study the desired robustness as provided by Figures 20-22 for all the examples. In Figure 20, sensitivity plots portraying variations in plant parameters for example-1 are displayed. Maximum sensitivity is a robustness measure which is expected to be below 2 (or 6dB) for stable systems [29]. The Bode magnitude plot indicates that the system's sensitivity remains below $M_s = 2$ or 6dB even when subjected to a 40% variation in plant parameters. Similarly, Figures 21 and 22 exhibit sensitivity plots for plant parameter variations in examples 2 and 3, respectively. These plots corroborate similar observations to those evident in Figure 20. Observing these figures, it can be concluded that the fractional dual-tilt control scheme guarantees robust stability even for 40% variation in plant parameters.

2) ROBUSTNESS CHECK AMID DIFFERENT LEVELS OF PERTURBATION

To verify actual perturbations to plant parameters (K and L), the outputs are plotted for all three examples in Figures 23 to 28. In this critical verification, perturbations in K and L are applied separately and gradually increased until they deliver acceptable performance. For example-1, robustness analysis amid different levels of perturbation (in

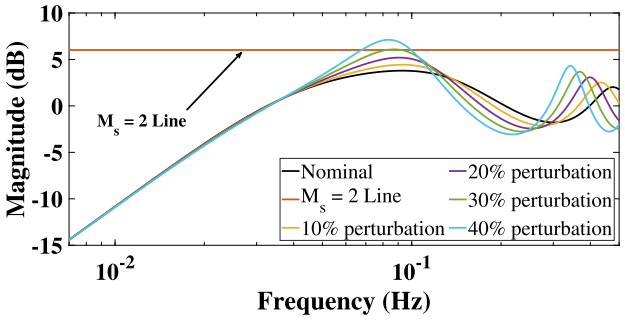

FIGURE 22. Sensitivity plots with respect to plant parameter variations for example-3.

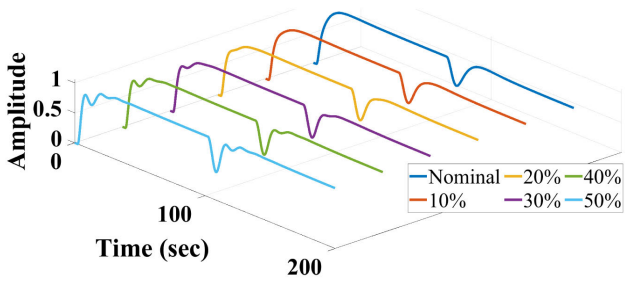

FIGURE 23. Robustness analysis when perturbation in system gain *K* for example-1.

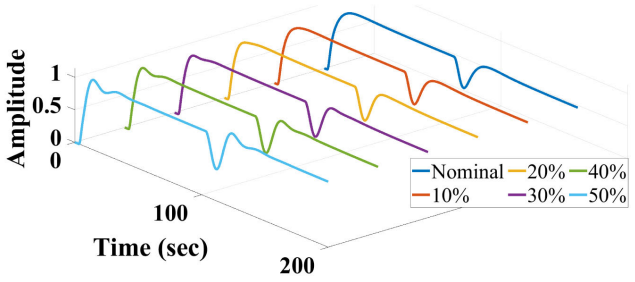

FIGURE 24. Robustness analysis when perturbation in system delay *L* for example-1.

system gain (K) and system delay (L)) are presented in Figures 23 and 24, respectively. Likewise, for example-2, robustness assessment is carried out amid different levels of perturbation in K and L. The resulting closed-loop responses are shown in Figures 25 and 26. Finally, for example-3, the robustness analysis is presented in Figures 27 and 28, showcasing system behavior under perturbations in K and L. The robustness check carried out in all three examples reveals that the proposed design has the capacity to withstand up to 50% perturbations while maintaining stable closed-loop responses. Interestingly, the observation was true for all examples studied. It demonstrates that the presented structure can be robust even with large plant parameter variations. The method has obtained comparable stability with almost no significant changes in time responses. Thus, it depicts the

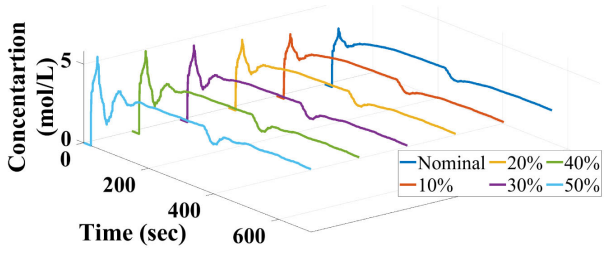

FIGURE 25. Robustness analysis when perturbation in system gain *K* for example-2.

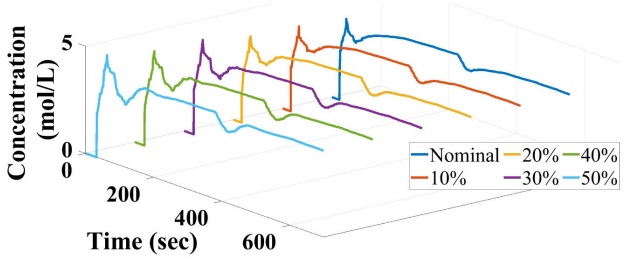

FIGURE 26. Robustness analysis when perturbation in system delay *L* for example-2.

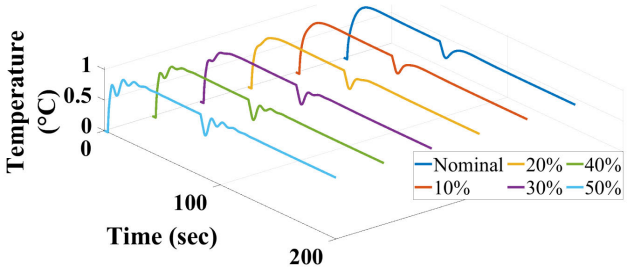

FIGURE 27. Robustness analysis when perturbation in system gain *K* for example-3.

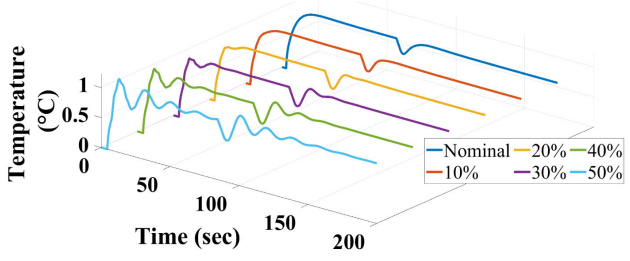

FIGURE 28. Robustness analysis when perturbation in system delay *L* for example-3.

new $\text{FOT}^{\alpha}\text{D}^{1-\alpha}$ controller can be designed robustly using GM-PM effectively and with less computational burden.

E. COMMENTS ON STABILITY

In pursuit of optimal closed-loop stability, the scheme $\text{FOT}^{\alpha}\text{D}^{(1-\alpha)}$ performs superior and robust. It can provide a favourable balance between performance and robustness.

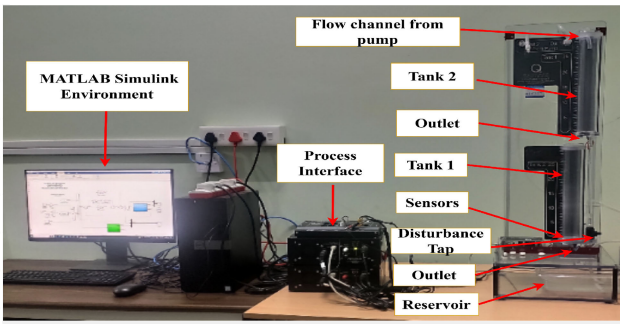

FIGURE 29. Experimental arrangement of a two-tank system.

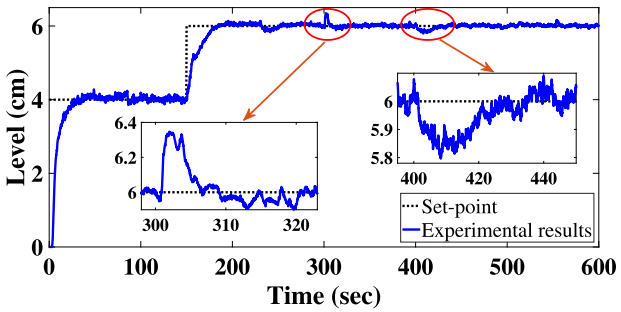

FIGURE 30. Experimental Outcomes.

Additionally, introducing a 'tilt' term extends the overall bandwidth and contributes to the overall performance. Within the 2DOF framework, where uncertainties are inherent in most industrial processes, and variations in plant parameters are common, robust stability becomes a critical consideration. The proposed design is meticulously developed to ensure robust stability, considering recommended stability margins. It is proven through rigorous assessments in three illustrative examples. Encouragingly, the responses obtained in all cases demonstrate high satisfaction.

V. EXPERIMENTAL VALIDATION ON A TWO-TANK LEVEL CONTROL SYSTEM

Figure 29 shows the experimental setup of a two-tank level control system. Here, water from the reservoir is pumped to tank-2, and again water from tank-2 is forwarded to tank-1. In this process, the main objective is to control the level of tank-1 by regulating the pump voltage. Through system identification, an analogous pure integrating time-delayed system is estimated as $P(s) = \frac{0.1175e^{-3.5s}}{s}$. For the given plant, the values of $\lambda_{1,2}$ and $\alpha_{1,2}$ are obtained as 3.674 and 0.123, respectively, from the GM-PM constraints. The $\text{FOT}^{\alpha}\text{D}^{1-\alpha}$ controller transfer functions are obtained as $\frac{1.1582}{s^{0.1230}} + 1.9259s^{0.877}$. The experiment had a target level set to 4 cm at 0 sec and VI cm at 150 sec. A manual output disturbance is applied by injecting a very small amount of water at 300 sec, and an input disturbance is applied by opening the disturbance tap at 400 sec. The actual output and the corresponding control signal are plotted in

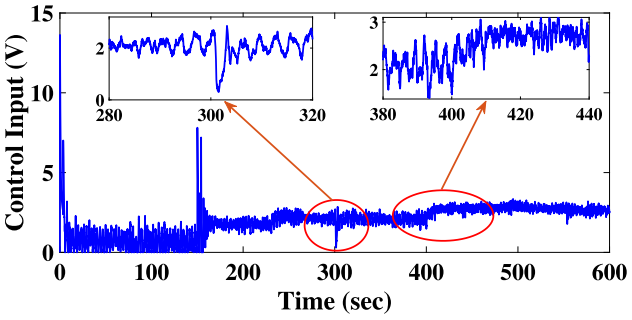

FIGURE 31. Control signal.

Figures 30 and 31, respectively. Figures 30 and 31 show the proposed design's set-point tracking and load-disturbance rejection capabilities. Moreover, this verification demonstrates that the novel controller can operate in real-time with satisfactory performance.

VI. CONCLUSION

A fractional dual-parametric robust predictive control strategy was presented for integrating processes with time delays. The new control structure involving $\text{FOT}^{\alpha}\text{D}^{1-\alpha}$, offered improved set-point tracking and load disturbance rejections on well-known benchmark plants. With simple computational effort, the designed parameters can be calculated to achieve a tolerance of up to 30% or even more parametric uncertainties. While considering the previous designs on FOCs, the present design is relatively straightforward to apply. Also, the effectiveness of the presented scheme was verified on the two-tank level control system.

REFERENCES

[1] S. Chakraborty, S. Ghosh, and A. Kumar Naskar, "I–PD controller for integrating plus time-delay processes," *IET Control Theory Appl.*, vol. 11, no. 17, pp. 3137–3145, Sep. 2017.
[2] D. Das, S. Chakraborty, and A. K. Naskar, "Controller design on a new 2DOF PID structure for different processes having integrating nature for both the step and ramp type of signals," *Int. J. Syst. Sci.*, vol. 54, no. 7, pp. 1423–1450, May 2023.
[3] S. Chakraborty, S. Ghosh, and A. K. Naskar, "All-PD control of pure integrating plus time-delay processes with gain and phase-margin specifications," *ISA Trans.*, vol. 68, pp. 203–211, May 2017.
[4] U. M. Nath, C. Dey, and R. K. Mudi, "Desired characteristic equation based PID controller tuning for lag-dominating processes with real-time realization on level control system," *IEEE Control Syst. Lett.*, vol. 5, no. 4, pp. 1255–1260, Oct. 2021.
[5] S. R. Mahapatro and B. Subudhi, "A robust stability region-based decentralized PI controller for a multivariable liquid level system," *IEEE Syst. J.*, vol. 16, no. 1, pp. 124–131, Mar. 2022.
[6] F. Peker and I. Kaya, "Maximum sensitivity (Ms)-based I-PD controller design for the control of integrating processes with time delay," *Int. J. Syst. Sci.*, vol. 54, no. 2, pp. 313–332, Jan. 2023.
[7] F. Alyoussef and I. Kaya, "Simple PI-PD tuning rules based on the centroid of the stability region for controlling unstable and integrating processes," *ISA Trans.*, vol. 134, pp. 238–255, Mar. 2023.
[8] G. Lloyds Raja and A. Ali, "New PI-PD controller design strategy for industrial unstable and integrating processes with dead time and inverse response," *J. Control, Autom. Electr. Syst.*, vol. 32, no. 2, pp. 266–280, Apr. 2021.
[9] D. Das, S. Chakraborty, and G. L. Raja, "Enhanced dual-DOF PI-PD control of integrating-type chemical processes," *Int. J. Chem. React. Eng.*, vol. 21, no. 7, pp. 907–920, Jul. 2023.

[10] I. Kaya and F. Peker, "Optimal I-PD controller design for setpoint tracking of integrating processes with time delay," *IET Control Theory Appl.*, vol. 14, no. 18, pp. 2814–2824, Dec. 2020.

[11] K. Kothari, U. Mehta, and R. Prasad, "Fractional-order system modeling and its applications," *J. Eng. Sci. Technol. Rev.*, vol. 12, no. 6, pp. 1–10, Nov. 2019.

[12] P. Chen and Y. Luo, "Analytical fractional-order PID controller design with Bode's ideal cutoff filter for PMSM speed servo system," *IEEE Trans. Ind. Electron.*, vol. 70, no. 2, pp. 1783–1793, Feb. 2023.

[13] R. Singh, T. Dora, R. Lamba, A. K. Bhullar, and S. Sondhi, "FOPID controller design for a perturbed PHWR system using enhanced crow search algorithm," *Prog. Nucl. Energy*, vol. 151, Sep. 2022, Art. no. 104342.

[14] R. Trivedi and P. K. Padhy, "Design of indirect fractional order IMC controller for fractional order processes," *IEEE Trans. Circuits Syst. II, Exp. Briefs*, vol. 68, no. 3, pp. 968–972, Mar. 2021.

[15] R. Mondal and J. Dey, "A novel design methodology on cascaded fractional order (FO) PI-PD control and its real time implementation to cart-inverted pendulum system," *ISA Trans.*, vol. 130, pp. 565–581, Nov. 2022.

[16] V. P. Shankaran, S. I. Azid, and U. Mehta, "Fractional-order PI plus D controller for second-order integrating plants: Stabilization and tuning method," *ISA Trans.*, vol. 129, pp. 592–604, Oct. 2022.

[17] V. P. Shankaran, S. I. Azid, U. Mehta, and A. Fagiolini, "Improved performance in quadrotor trajectory tracking using MIMO PIλ-D control," *IEEE Access*, vol. 10, pp. 110646–110660, 2022.

[18] U. Mehta, P. Aryan, and G. L. Raja, "Tri-parametric fractional-order controller design for integrating systems with time delay," *IEEE Trans. Circuits Syst. II, Exp. Briefs*, vol. 70, no. 11, pp. 4166–4170, 2023, doi: 10.1109/TCSII.2023.3269819.

[19] F. Alyoussef and I. Kaya, "Improved adaptive dynamic non-singular terminal sliding mode controller with fractional disturbance observer," *Inf. Sci.*, vol. 641, Sep. 2023, Art. no. 119110.

[20] A. Ranjan and U. Mehta, "Fractional filter IMC-TDD controller design for integrating processes," *Results Control Optim.*, vol. 8, Sep. 2022, Art. no. 100155.

[21] A. Ranjan and U. Mehta, "Fractional-order tilt integral derivative controller design using IMC scheme for unstable time-delay processes," *J. Control, Autom. Electr. Syst.*, vol. 34, no. 5, pp. 907–925, Oct. 2023.

[22] A. Daraz, S. A. Malik, A. T. Azar, S. Aslam, T. Alkhalifah, and F. Alturise, "Optimized fractional order integral-tilt derivative controller for frequency regulation of interconnected diverse renewable energy resources," *IEEE Access*, vol. 10, pp. 43514–43527, 2022.

[23] U. Raj and R. Shankar, "Optimally enhanced fractional-order cascaded integral derivative tilt controller for improved load frequency control incorporating renewable energy sources and electric vehicle," *Soft Comput.*, vol. 27, no. 20, pp. 15247–15267, Oct. 2023.

[24] K. Singh, M. Amir, F. Ahmad, and M. A. Khan, "An integral tilt derivative control strategy for frequency control in multimicrogrid system," *IEEE Syst. J.*, vol. 15, no. 1, pp. 1477–1488, Mar. 2021.

[25] Y. Sun, J. Xu, G. Lin, W. Ji, and L. Wang, "RBF neural network-based supervisor control for Maglev vehicles on an elastic track with network time delay," *IEEE Trans. Ind. Informat.*, vol. 18, no. 1, pp. 509–519, Jan. 2022.

[26] Y. Sun, S. Wang, Y. Lu, J. Xu, and S. Xie, "Control of time delay in magnetic levitation systems," *IEEE Magn. Lett.*, vol. 13, pp. 1–5, 2022.

[27] K. Gnaneshwar and P. K. Padhy, "Robust design of tilted integral derivative controller for non-integer order processes with time delay," *IETE J. Res.*, vol. 69, no. 9, pp. 6198–6209, Sep. 2023.

[28] D. Mukherjee, G. L. Raja, P. Kundu, and A. Ghosh, "Improved fractional augmented control strategies for continuously stirred tank reactors," *Asian J. Control*, vol. 25, no. 3, pp. 2165–2182, May 2023.

[29] G. L. Raja and A. Ali, "Enhanced tuning of Smith predictor based series cascaded control structure for integrating processes," *ISA Trans.*, vol. 114, pp. 191–205, Aug. 2021.

[30] A. Ranjan, U. Mehta, and S. Saxena, "A comprehensive review of modified internal model control (IMC) structures and their filters for unstable processes," *Annu. Rev. Control*, vol. 56, May 2023, Art. no. 100895.

[31] C. Anil and R. Padma Sree, "Tuning of PID controllers for integrating systems using direct synthesis method," *ISA Trans.*, vol. 57, pp. 211–219, Jul. 2015.

[32] S. Kumari, P. Aryan, and G. L. Raja, "Design and simulation of a novel FOIMC-PD/P double-loop control structure for CSTRs and bioreactors," *Int. J. Chem. React. Eng.*, vol. 19, no. 12, pp. 1287–1303, Dec. 2021.

DIPJYOTI DAS (Graduate Student Member, IEEE) received the B.Tech. degree in electronics and instrumentation engineering from the National Institute of Technology Silchar, India, in 2017, and the M.Tech. degree from the Sant Longowal Institute of Engineering and Technology, Punjab, India, in 2020. He is currently pursuing the Ph.D. degree in electronics and instrumentation engineering with the National Institute of Technology Silchar.

SUDIPTA CHAKRABORTY received the M.Tech. and Ph.D. degrees in electrical engineering from the National Institute of Technology Rourkela, India. Currently, he is an Assistant Professor with the Electronics and Instrumentation Engineering Department, National Institute of Technology Silchar. His research interests include process control, PID control, time-delay, and fractional order systems.

UTKAL MEHTA (Senior Member, IEEE) received the Ph.D. degree in system identification and process control from IIT Guwahati, India. He is currently an Associate Professor in electrical and electronics engineering with The University of the South Pacific, Fiji. His current research interests include process identification, applied fractional calculus for modeling, and fractional-order filter design on re-configurable devices, such as FPGA, FPAA, and various robotics applications for medical and industrial automation.

G. LLOYDS RAJA (Member, IEEE) received the bachelor's degree in electronics and communication engineering and the master's degree in embedded system technologies from Anna University, in 2009 and 2011, respectively, and the Ph.D. degree from the Electrical Engineering Department, Indian Institute of Technology Patna, in 2018. From 2017 to 2020, he was an Assistant Professor with the Kalinga Institute of Industrial Technology. He visited the Department of Automation, Shanghai Jiao Tong University, China, as a Postdoctoral Researcher, for a short duration. Since 2020, he has been with the Electrical Engineering Department, National Institute of Technology Patna, where he is currently an Assistant Professor. His current research interests include chemical process control, advanced load frequency control strategies, adaptive control, and applications of metaheuristic optimization techniques for controller tuning. He is also a member of IFAC-ACDOS.